Canine ependymoma: Diagnostic criteria and common pitfalls

Andrew D. Miller[1], Jennifer W. Koehler, Taryn A. Donovan, Jennifer E. Stewart, Brian F. Porter, Daniel R. Rissi, Simon L. Priestnall, F. Yvonne Schulman

Department of Biomedical Sciences, Section of Anatomic Pathology, Cornell University College of Veterinary Medicine, Ithaca, NY (AM); Department of Pathobiology, Auburn University, College of Veterinary Medicine, Auburn, AL (JK); Department of Anatomic Pathology, The Animal Medical Center, New York, NY (TD); Animal Health Trust, Newmarket, United Kingdom (JS); Department of Veterinary Pathobiology, Texas A&M University, College Station, TX (BP); Athens Veterinary Diagnostic Laboratory and Department of Pathology, University of Georgia, College of Veterinary Medicine, Athens, GA (DR); Department of Pathobiology and Population Sciences, The Royal Veterinary College, Hatfield, United Kingdom (SP); Veterinary Services, Marshfield Labs, Marshfield, WI (YS)

[1]Corresponding Author: Andrew D. Miller, Cornell University, Department of Biomedical Sciences, Section of Anatomic Pathology, T5-006A Veterinary Research Tower, Ithaca, NY 14853. 607-253-3559 (phone), 607-253-3541 (fax), adm10@cornell.edu

Abstract

Reports of canine ependymoma are generally restricted to single case reports with tumor incidence estimated at 2-3% of primary central nervous system (CNS) tumors. While most commonly reported in the lateral ventricle, tumors can occur anywhere in the ventricular system and in extraventricular locations. Rosettes and pseudorosettes are a common histologic feature; however, these features can be mimicked by other CNS neoplasms. Thirty-seven potential ependymoma cases were identified in a retrospective database search of eight institutions, and a histologic review of all cases was conducted. Of thirty-seven cases, twenty-two candidate cases were further subjected to a consensus histologic and immunohistochemical review, and only 5/37 (13.5%) were conclusively identified as ependymoma. The neuroanatomic locations included lateral ventricle (3/5), third ventricle (1/5), and mesencephalic aqueduct (1/5). Subtypes included papillary (4/5) and tanycytic (1/5). Histologic features included rosettes (5/5), pseudorosettes (5/5), ependymal canals (2/5), tanycytic differentiation (1/5), blepharoplasts (1/5), ciliated cells (1/5), and high nuclear to cytoplasmic ratio (5/5). Immunolabeling for GFAP (4/4) and CKAE1/3 (3/4) was found in pseudorosettes, rosettes, and scattered individual neoplastic cells. Diffuse, but variably intense cytoplasmic S100 immunolabeling was detected in 3/4 cases. Olig2 intranuclear immunolabeling was observed in less than 1% of the neoplastic cells (3/3). Tumors that had pseudorosettes and mimicked ependymoma included oligodendroglioma, choroid plexus tumor, pituitary corticotroph adenoma, papillary meningioma, and suprasellar germ cell tumor. These findings indicate that canine ependymoma is an extremely rare neoplasm with histomorphologic features that overlap with other primary CNS neoplasms.

Keywords: Canine, brain, ependymoma, glioma, immunohistochemistry, meningioma, pseudorosette, rosette

Introduction

Ependymal cells are specialized ciliated epithelial cells that line the ventricular system. These cells are present throughout the central nervous system and perform a number of functions, including interaction with the subventricular zone during development and regulation of permeability to cerebrospinal fluid components.[3] The

ependyma consists of a single layer of cuboidal, ciliated cells that line the ventricles and a smaller population of specialized cells called tanycytes, which are most commonly located in the third ventricle and have long processes that interact with the adjacent neuroparenchyma.[3] In veterinary species, neoplasms with ependymal differentiation (ependymomas) are uncommon to rare with the incidence highest in cats.[18] In dogs, the incidence of ependymoma is difficult to determine due to limited scientific literature; however, one retrospective series reported only one case of ependymoma in 435 cases of intracranial neoplasia.[12] Other reports suggest an incidence of approximately 2-3% of all primary intracranial tumors in the dog.[15] Canine ependymoma is reported most frequently in the lateral and third ventricles and rarely in the spinal cord.[15] Regardless of location, tumors typically manifest grossly as a large, intraventricular mass that variably infiltrates and compresses the adjacent parenchyma.[9,14,15,17,19] Histologically, their appearance can be quite diverse, and subtypes include clear cell, papillary, and tanycytic.[9,14,15,17] Diagnosis is aided by the presence of perivascular pseudorosettes with anti-basilar nuclei and cytoplasmic processes that abut blood vessels; however, this pattern is not unique to ependymomas and can be easily misinterpreted. Immunohistochemistry and transmission electron microscopy can aid in the diagnosis, the latter used to confirm the presence of desmosomes and cilia. Herein, we describe a case series of canine ependymomas that was derived from a multi-board certified veterinary pathologist consensus review of cases previously diagnosed as ependymoma at respective institutions. Given the challenges in accurately diagnosing ependymoma based solely on histology, we briefly review the neoplasms that were misdiagnosed as ependymoma and provide diagnostic support for the alternate microscopic interpretations.

Materials and Methods

Biopsy and necropsy records for the New York State Animal Health Diagnostic Center, Cornell University College of Veterinary Medicine (1979-2015), University of Georgia Department of Pathology and Athens Veterinary Diagnostic Laboratory (2000-2015), Auburn University College of Veterinary Medicine, Department of Pathobiology (1996-2016), The Animal Medical Center, Department of Anatomic Pathology (1999-2015), Animal Health Trust (1990-2015), Texas A&M University College of Veterinary Medicine & Biomedical Sciences, Department of Veterinary Pathobiology (2002-2015), and The Royal Veterinary College, Department of Pathobiology and Population Sciences (1997-2017) were searched for cases of canine ependymoma. Additional select cases were provided from the Armed Forces Institute of Pathology archives by one co-author (YS). All cases that fit inclusion criteria (i.e. coded in the respective institutional computer system as ependymoma) were reviewed by all co-authors, and from this initial review, cases that were clearly not ependymoma based on inconsistent histologic features were removed from consideration. Consensus was based on at least 75% agreement amongst the reviewers. The following immunohistochemical stains were used: glial fibrillary acidic protein (GFAP; rabbit polyclonal, Agilent, Carpinteria, CA, catalog #Z0334), cytokeratin AE1/AE3 (CKAE1/3; mouse monoclonal, Agilent, catalog #MS351501-2), oligodendrocyte transcription factor 2 (Olig2; rabbit monoclonal, Abcam, Cambridge, MA, catalog #AB109186), S100 (rabbit polyclonal, Agilent, catalog #IS50430-2), and adrenocorticotropic hormone (ACTH; mouse monoclonal, Agilent, catalog #M350101-2). The stains were reviewed by the co-authors before coming to a consensus diagnosis. PTAH histochemical staining and ACTH immunohistochemistry were only performed on select cases based on the histologic

features, whereas GFAP, CKAE1/AE3, Olig2, and S100 were performed on all cases in which tissue was available.

PTAH staining was performed according to standard laboratory protocols. The following protocols were used for immunohistochemistry utilizing the Leica Bond Max Automated Immunohistochemistry Staining System, according to the manufacturer's instructions (Leica Microsystems, Illinois, United States). Briefly, tissues were sectioned at 5 μm and deparaffinized with Bond Dewax Solution (Leica, catalog #AR9222). Pretreatment with heat-induced antigen retrieval was performed for 30 minutes using Tris/EDTA pH 9 (Bond Epitope Retrieval Solution 2, Leica, catalog #AR9640) for CKAE1/3 and Olig2. No pretreatment was used for GFAP, S100, and ACTH. Endogenous peroxidase activity was blocked with a 3% peroxide solution for 5 minutes (Leica, catalog #DS9800). The antibodies were diluted at 1:500 for 15 minutes (GFAP), 1:200 for 60 minutes (CKAE1/3 and Olig2), 1:400 for 14 minutes (S100), and 1:200 for 30 minutes (ACTH). Biotin-free PowerVision poly-polymeric horseradish peroxidase anti-mouse (Leica, catalog #PV6114) or anti-rabbit (Leica, catalog #PV6119) IgG reagent was then applied to the slides for 30 minutes followed by incubation with Bond Polymer Refine Detection for 10 minutes (Leica, catalog #DS9800). Tissues were developed with 3,3-diaminobenzidine (DAB) (Leica, catalog #DS9800) for 10 minutes. The slides were counterstained with hematoxylin (Leica, catalog #DS9800) for 5 minutes, dehydrated, cleared, and mounted. Positive controls consisted of normal canine brain (GFAP, Olig2, and S100), small intestine (CKAE1/3), and pituitary gland (ACTH). Negative controls consisted of an isotype-matched antibody.

Results

Thirty-seven cases were originally identified by computer search and after initial histologic review, twenty-two cases (60%) had histologic features potentially consistent with ependymoma and therefore were included for further analysis. Of the fifteen cases that were not subject to further review, diagnoses included oligodendroglioma (6/15), pituitary adenoma (3/15), astrocytoma (3/15), nephroblastoma (1/15), meningioma (1/15), and non-diagnostic (1/15). Of the twenty-two cases reviewed for consensus diagnosis, only 5/22 (22.7%) were diagnosed as ependymoma based on the combination of histologic, histochemical, and immunohistochemical features. Breed, sex, age, tumor location, and tumor subtype are described in Table 1. Four of the cases were classified as papillary ependymomas and one as a tanycytic ependymoma. Papillary ependymomas were characterized by cords, ribbons, and papilliform projections of neoplastic ependymal cells that had moderate amounts of cytoplasm and round to ovoid nuclei with a dense chromatin pattern (Fig. 1). All ependymomas had rosettes (5/5) and pseudorosettes (5/5) (Figs. 2-3). Rosettes often contained intraluminal, pale basophilic material (Fig. 3). The single case of ependymoma with tanycytic differentiation had elongated cells with flattened, spindled nuclei (Fig. 4). Fewer cases had ependymal canals (2/5), blepharoplasts (1/5), and ciliated cells (1/5) (Fig. 5). One case had clear progression from a thickened, dysplastic ependyma (Fig. 6). A high nuclear to cytoplasmic ratio (5/5) and areas of necrosis (3/5) were features in a majority of cases. Hemorrhage, microvascular proliferation, and areas of calcification were absent in all cases. Atypia was moderate in all cases and the mitotic rate was less than one per 400x field (2.37 mm^2) in all cases. Multifocal cytoplasmic staining for PTAH was present in the one case in which this stain was used. Strong cytoplasmic immunolabeling for GFAP (4/4) was found in

pseudorosettes (Fig. 7), rosettes, and in up to 60% of the neoplastic cells not forming pseudorosettes or rosettes (Fig. 8). Strong cytoplasmic immunolabeling to CKAE1/3 (3/4) generally mirrored the GFAP staining and was found in pseudorosettes, rosettes (Fig. 9), and scattered individual neoplastic cells (Fig. 10). The staining intensity for CKAE1/3 was greater in the rosettes than the GFAP immunolabeling. Olig2 intranuclear immunolabeling was seen in less than 1% of the neoplastic cells (3/3) (Fig. 11). Diffuse, but variable, cytoplasmic S100 immunolabeling was detected in 3/4 cases (Fig. 12).

Of the remaining potential 17 cases, the following diagnoses were made with the addition of immunohistochemical stains coupled with the histologic features: oligodendroglioma (6/17), choroid plexus tumor (5/17), pituitary corticotroph adenoma (4/17), meningioma (1/17) and suprasellar germ cell tumor (1/17). All cases of oligodendroglioma were either primary intraventricular neoplasms or arose periventricularly and extended into the ventricular system. Oligodendrogliomas were characterized by sheets of round to ovoid neoplastic cells with a variable amount of cytoplasm, round, sometimes molded, nuclei, and a variable chromatin pattern. All cases had a significant number of pseudorosettes (Fig. 13), and diffuse intranuclear Olig2 immunolabeling was present in nearly 100% of the neoplastic cells (Fig. 13, inset). Neoplastic oligodendrocytes lacked immunolabeling for GFAP and CKAE1/3 and had variable cytoplasmic immunolabeling for S100.

All cases diagnosed as choroid plexus tumors were primary intraventricular masses composed of dense cords, interlacing tubular structures, and pseudorosettes of neoplastic epithelial cells (Fig. 14). Typical papillary and villiform projections common in most canine choroid plexus tumors were lacking in many of these tumors. CKAE1/3 was diffusely positive in all neoplastic cells of the choroid

plexus tumors with strong intracytoplasmic immunolabeling (Fig. 14, inset). Choroid plexus tumors lacked immunolabeling for GFAP, Olig2, and S100.

The pituitary tumors were entirely restricted to the third ventricle, bulging into and compressing the thalamus. These tumors were composed of tubules, rosettes, pseudorosettes, and loose clusters of neuroendocrine-like epithelial cells (Fig. 15). All cases had rosettes containing basophilic material, mimicking the pattern seen in some ependymomas; however, no ciliated cells were present. All cases had robust and diffuse intracytoplasmic immunolabeling for ACTH (Fig. 15, inset). CKAE1/3 immunolabeling in the pituitary tumors was robust and nearly diffuse, and patchy to diffuse cytoplasmic S100 immunolabeling was present. Pituitary tumors lacked immunolabeling for GFAP and Olig2.

For the meningioma case, characteristic meningothelial whorls were present; however, a majority of the neoplasm was composed of prominent pseudorosettes of meningothelial cells typical for the papillary subtype of meningioma (Fig. 16). Lastly, the germinoma case consisted of a multiphasic neoplasm composed of germ-like cells admixed with a neuroparenchyma-like stroma. While rare pseudorosettes were noted in the germinoma, the histology was distinct from that seen in ependymomas. Immunohistochemistry was not deemed necessary to diagnose the meningioma or germinoma case.

Discussion

Ependymomas are an uncommon to rare glioma in the dog that are most frequently reported in the lateral and third ventricles.[15] While the cell of origin in the dog is not known, studies of human ependymoma reveal features of radial glia, a neural stem cell that resides in the subventricular zone.[4] Ependymomas are typically well-circumscribed intraventricular neoplasms that do not extend extensively into the

adjacent parenchyma. Pseudorosettes and rosettes are an important histologic feature of these tumors; however, they are not specific to ependymomas and utilizing them as the sole criterion for ependymoma diagnosis is ill advised, supported by the findings in this study. Important histologic features that are specific to ependymomas include ependymal canals (linear spaces lined by neoplastic ependymal cells), ciliated epithelial cells lining the rosettes, and blepharoplasts (basal ciliary bodies identified by PTAH histochemical staining).[7] As demonstrated here, the diagnosis can be greatly aided by immunohistochemistry, which typically relies on GFAP immunolabeling in pseudorosettes and other parts of the tumor, multifocal pan-cytokeratin immunolabeling in pseudorosettes, rosettes, and other tumor cells, and sparse Olig2 immunolabeling. Human ependymomas commonly express vimentin and S100 and rarely express neuronal antigens.[5,16] While the underlying molecular abnormalities associated with ependymoma in humans are well described and include mutational activation of MAPK, PDGFR, and VEGF, the rarity of these tumors in the dog has limited molecular characterization.[1,13]

The current case series details the collective efforts and consensus review of eight board-certified veterinary pathologists, all of whom have extensive experience and expertise with diagnostic veterinary neuropathology. Of the thirty-seven cases originally selected from archival searches, only five were confirmed as ependymoma based on histology with or without immunohistochemical features. Based on the small number of cases, no breed or sex predilection can be determined, and the tumors were most common in middle-aged dogs. Three cases involved the lateral ventricle, consistent with the predilection sites recorded in the literature. While pseudorosettes and rosettes were present in all cases, other more specific features of ependymoma (ependymal canals, ciliated cells, and blepharoplasts) were present

in a minority of cases. Four of the cases were diagnosed as papillary ependymomas, whereas one had tanycytic features. Most reported cases of canine ependymoma are papillary subtypes, with rare reports of clear cell and anaplastic variants.[9,14,17,19]

The inclusion of immunohistochemistry can greatly aid in the diagnosis of ependymoma; however, it must be interpreted in context with the expected staining patterns of other intracranial neoplasms in the dog. In the current cases series, GFAP was immunoreactive in all of the ependymoma cases in which tissue was available. Immunolabeling was strong in the cells forming the pseudorosettes and rosettes, as well as in single to small clusters of neoplastic cells throughout the neoplasm. While GFAP is traditionally used to label cells of astrocytic origin, it is also normally expressed in ependyma and radial glial cells, making GFAP expression useful in the diagnosis of ependymoma.[6,19] In these canine ependymomas, GFAP was robustly expressed in pseudorosettes and to a lesser degree in rosettes. A similar pattern of immunolabeling was noted for pan-cytokeratin, although immunolabeling was often more robust in the rosettes compared to GFAP. Cytokeratin expression occurs in the vast majority of ependymomas, but it can be widely variable in intensity, ranging from scant immunolabeling to marked immunolabeling noted in the pseudorosettes and rosettes.[16,18] Importantly, Olig2 immunolabeling was extremely limited. This is consistent with the staining pattern of Olig2 in human ependymomas, in which a minor subset of neoplastic cells has expression of Olig2. [4,5] Since this pattern of Olig2 expression is expected with radial glia, it is often used to support the contention that these tumors arise from a subpopulation of radial glia stem cells.[4,5] S100 immunolabeling was present in 3/4 of the cases, and while certainly not specific to ependymoma, the multifocal, intense

cytoplasmic staining pattern was consistent with that reported in human ependymoma.[16]

The presence of pseudorosettes and rosettes can lead to a diagnostic dilemma, as these are features that can be recapitulated in a number of primary intracranial neoplasms in the dog. In the current consensus series, previously diagnosed ependymomas were reclassified as oligodendroglioma, choroid plexus tumor, pituitary adenoma, meningioma, and suprasellar germinoma.

In the dog, gliomas are the second most common primary intracranial tumor, with oligodendrogliomas having an incidence of up to 70%.[8] Oligodendrogliomas have relatively uniform cellularity and are composed of round to polygonal cells with round to ovoid nuclei, finely stippled chromatin, and inapparent nucleoli. The presence of pseudorosettes can be sporadic or abundant in these tumors and can lead to diagnostic confusion when the tumor is located within a ventricle.[8,11] Oligodendrogliomas can have extensive ventricular involvement; however, to differentiate ependymoma from oligodendroglioma, several features can be used. The presence of the characteristic “fried-egg” autolytic histologic pattern, the “chicken wire” vascular pattern, myxoid stroma, nuclear rowing or molding, and coarse nuclear chromatin can be used to help distinguish oligodendrogliomas from ependymomas. Importantly, Olig2 immunolabeling is typically present in the majority of neoplastic cells in oligodendrogliomas, in contrast to the pattern observed in ependymomas.[8]

Choroid plexus tumors represent approximately 10% of primary intracranial tumors in the dog.[15] They arise from the choroid plexus epithelium, occurring predominately in the lateral ventricles and fourth ventricles with occasional spread to other regions of the ventricular system. Most canine choroid plexus tumors are

formed by papillary projections of choroid plexus epithelium supported by a fine fibrovascular stroma, but other patterns include tubular-like differentiation, acinar-like structures, and sheet-like growth of cuboidal epithelial cells. The small acinar-like structures have a central fibrovascular core and mimic a pseudorosette. Unlike ependymomas, these tumors are diffusely immunolabeled with pan-cytokeratin and lack immunolabeling for Olig2 and GFAP. Other more specific antibodies to the choroid plexus, including Kir7.1, E-cadherin, and N-cadherin, can be used to further justify the diagnosis of choroid plexus tumors in the dog.[2,10]

Pituitary gland tumors can invade dorsally to involve the third ventricle and the surrounding brain parenchyma. Corticotroph tumors are relatively common in the dog and can either be functional or non-functional. Pituitary tumors that include rosettes and pseudorosettes can easily be confused with ependymomas, but while the histologic pattern may be similar in some respects, the immunohistochemical staining patterns are vastly different. Pituitary tumors have abundant immunolabeling for pan-cytokeratin and ACTH and are not expected to have immunolabeling for GFAP and Olig2.

Meningiomas, due to their neuroectodermal lineage, can produce a wide variety of histologic patterns, but meningothelial whorls are a defining feature, even when rarely present within the neoplasm. In addition, the nuclei of meningiomas are large with an open chromatin pattern, which is distinct from other primary intracranial neoplasms. The papillary subtype of meningioma is the most problematic, as it presents with abundant pseudorosettes that can mimic those seen in ependymomas. However, the location of the tumor (extra-axial), as well as the presence of meningothelial whorls, aids in the diagnosis. There are no immunohistochemical

stains that are definitive for canine meningioma, but meningiomas lack immunolabeling for Olig2 and can have patchy immunolabeling for pan-cytokeratin.[6]

Lastly, germinomas arising in the suprasellar region can invade the third ventricle and mimic ependymoma. These tumors have a distinct histomorphology composed of clusters, sheets, and islands of germ cells, often with epithelial and hepatocyte-like differentiation. Suprasellar germ cell tumors strongly express alpha-fetoprotein; however, complete immunohistochemical studies of these tumors have not been performed in the dog.

In conclusion, ependymomas are rare tumors in the dog. While pseudorosettes and rosettes are characteristic features of ependymomas, they are not pathognomonic. The tumor location (intraventricular), other histologic features (ependymal canals, ciliated epithelial cells lining the rosettes, and blepharoplasts), histochemical stains (PTAH), and immunohistochemistry (GFAP, pan-cytokeratin, Olig2) can help differentiate ependymomas from other primary brain tumors.

Acknowledgments

The authors thank the histopathology technicians at the Cornell University College of Veterinary Medicine, New York State Animal Health Diagnostic Center for assistance with case processing and Jen Patterson for assistance with images. The authors thank Dr. Brad Njaa for submitting case 5 for review.

Declaration of conflicting interests

The author(s) declared no potential conflicts of interest with respect to the research, authorship, and/or publication of this article.

Funding

The author(s) declared that they received no financial support for their research and/or authorship of this article.

References

1 Chiang JC, Ellison DW. Molecular pathology of paediatric central nervous system tumours. *J Pathol* 2017;241(2):159-172.

2 Choi EJ, Sloma EA, Miller AD. Kir7.1 immunoreactivity in canine choroid plexus tumors. *J Vet Diagn Invest* 2016;28(4):464-468.

3 Del Bigio MR. Ependymal cells: biology and pathology. *Acta Neuropathol* 2010;119(1):55-73.

4 Dorfer C, Tonn J, Rutka JT. Ependymoma: a heterogeneous tumor of uncertain origin and limited therapeutic options. *Handb Clin Neurol* 2016;134:417-431.

5 Ellison DW, McLendon R, Wiestler OD, et al. Ependymoma. In: Louis DN, Ohgaki H, Wiestler OD, Cavenee WK, Ellison DW, Figarella-Branger D, Perry A, Reifenberger G, von Deimling A, ed. *WHO Classification of Tumors of the Central Nervous System*. Lyon, France: International Agency for Research on Cancer; 2016:106-112.

6 Johnson GC, Coates JR, Wininger F. Diagnostic immunohistochemistry of canine and feline intracalvarial tumors in the age of brain biopsies. *Vet Pathol* 2014;51(1):146-160.

7 Kawano N, Yagishita S, Hara M, Tadokoro M. Pathologic features of ependymoma: Histologic patterns and a review of the literature. *Neuropathology* 1998;18:1-12.

8 Koehler JW, Miller AD, Miller CR, et al. A Revised Diagnostic Classification of Canine Glioma: Towards Validation of the Canine Glioma Patient as a Naturally Occurring Preclinical Model for Human Glioma. *J Neuropathol Exp Neurol* 2018;77(11):1039-1054.

9 Michimae Y, Morita T, Sunagawa Y, Sawada M, Okamoto Y, Shimada A. Anaplastic ependymoma in the cervical spinal cord of a maltese dog. *J Vet Med Sci* 2004;66(9):1155-1158.

10 Reginato A, Girolami D, Menchetti L, Foiani G, Mandara MT. E-cadherin, N-cadherin Expression and Histologic Characterization of Canine Choroid Plexus Tumors. *Vet Pathol* 2016;53(4):788-791.

11 Rissi DR, Levine JM, Eden KB, et al. Cerebral oligodendroglioma mimicking intraventricular neoplasia in three dogs. *J Vet Diagn Invest* 2015;27(3):396-400.

12 Song RB, Vite CH, Bradley CW, Cross JR. Postmortem evaluation of 435 cases of intracranial neoplasia in dogs and relationship of neoplasm with breed, age, and body weight. *J Vet Intern Med* 2013;27(5):1143-1152.

13 Thomson SA, Kennerly E, Olby N, et al. Microarray analysis of differentially expressed genes of primary tumors in the canine central nervous system. *Vet Pathol* 2005;42(5):550-558.

14 Traslavina RP, Kent MS, Mohr FC, et al. Clear cell ependymoma in a dog. *J Comp Pathol* 2013;149(1):53-56.

15 Vandevelde M, Higgins RJ, Oevermann A. *Veterinary Neuropathology: Essentials of Theory and Practice*. Oxford, UK: Wiley-Blackwell, 2012.

16 Vege KD, Giannini C, Scheithauer BW. The immunophenotype of ependymomas. *Appl Immunohistochem Mol Morphol* 2000;8(1):25-31.

17 Vural SA, Besalti O, Ilhan F, Ozak A, Haligur M. Ventricular ependymoma in a German Shepherd dog. *Vet J* 2006;172(1):185-187.

18 Woolford L, de Lahunta A, Baiker K, Dobson E, Summers BA. Ventricular and extraventricular ependymal tumors in 18 cats. *Vet Pathol* 2013;50(2):243-251.

19 Zachary JF, O'Brien DP, Ely RW. Intramedullary spinal ependymoma in a dog. *Vet Pathol* 1981;18(5):697-700.

Figure legends

Figures 1-6. Brain, canine ependymoma, hematoxylin and eosin (HE). **Figure 1.** Case 1. Rosettes (arrow) and pseudorosettes (asterisk) are common. **Figure 2.** Case 2. Elongate ribbons of neoplastic ependymal cells lining open spaces consistent with ependymal canals (arrows). **Figure 3.** Case 4. Rosettes either have empty lumina or contain basophilic material (arrow). **Figure 4.** Case 2. Elongated neoplastic cells consistent with tanycytic differentiation forming pseudorosettes. **Figure 5.** Case 4. Rare rosettes are lined by ciliated ependymal cells. **Figure 6.** Case 5. Neoplastic cells emerge from a thickened, dysplastic ependymal lining. Lateral ventricle lumen denoted by asterisk.

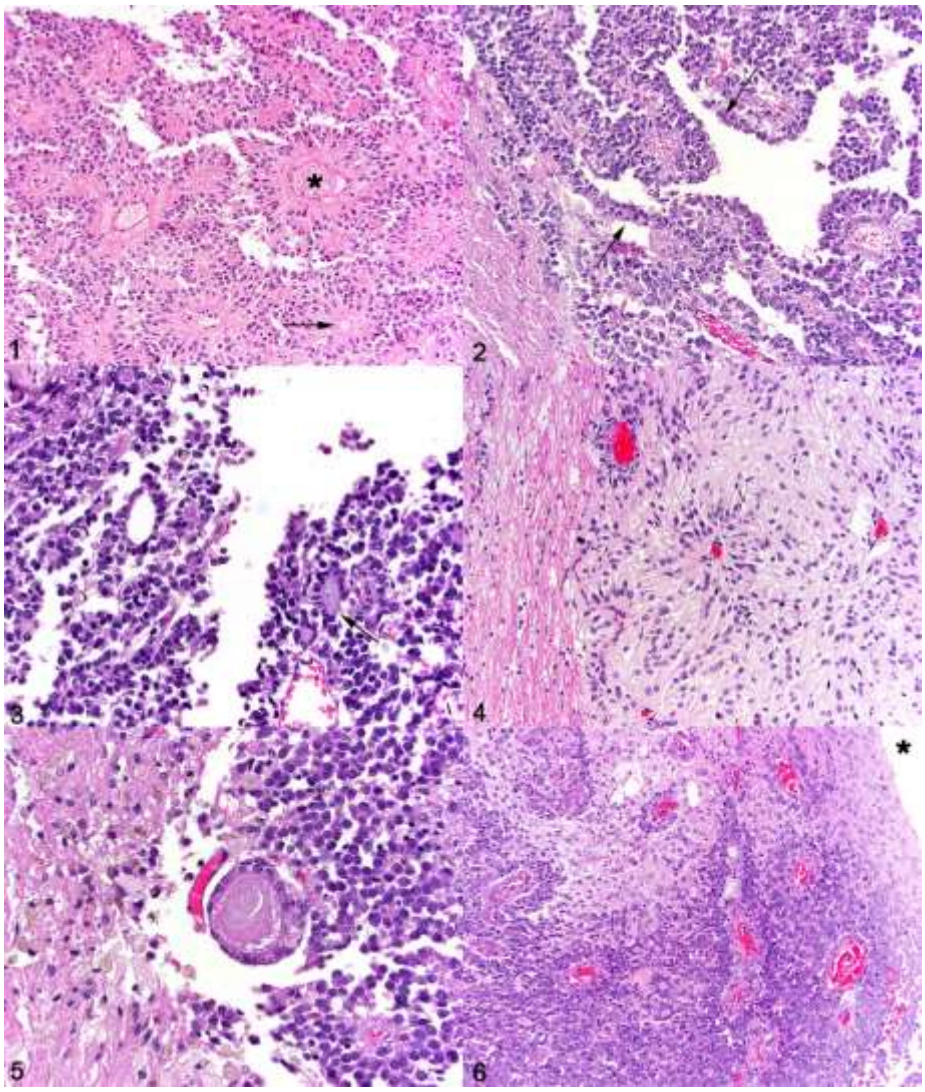

Figure 7-12. Brain, canine ependymoma, immunohistochemistry (IHC). **Figure 7.** Case 1. GFAP immunolabeling is consistently localized to the processes of neoplastic cells that abut blood vessels (pseudorosettes). **Figure 8.** Case 2. Neoplastic cells have strong cytoplasmic immunolabeling for GFAP. **Figure 9.** Case 4. CKAE1/3 immunolabeling is intense in rosettes and pseudorosettes. **Figure 10.** Case 2. Diffuse, but variably intense immunolabeling to CKAE1/3. **Figure 11.** Case 4. Intranuclear Olig2 immunolabeling is restricted to a small minority of cells (arrows). **Figure 12.** Case 2. Cytoplasmic S100 immunolabeling is strong and diffuse.

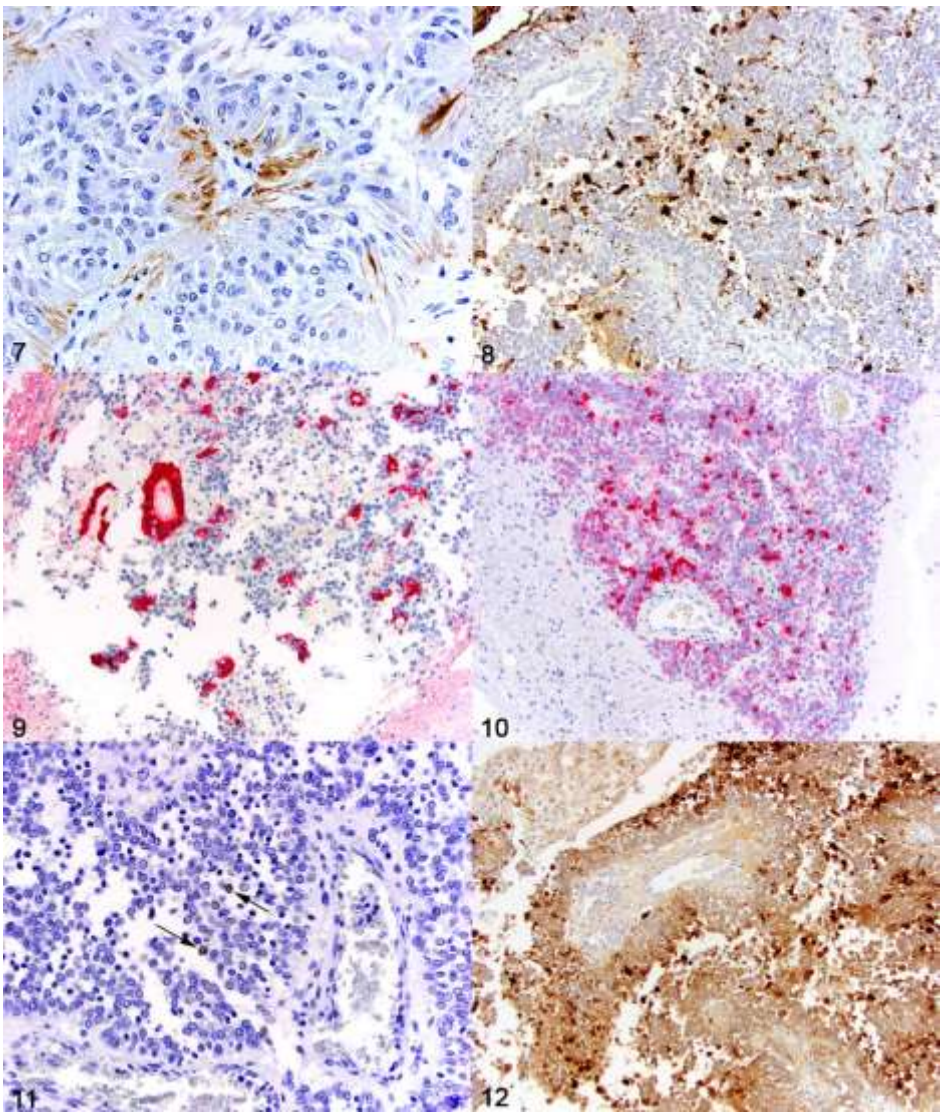

Figure 13-16. Brain, canine, mimics of canine ependymoma. **Figure 13.** Intraventricular oligodendroglioma composed of sheets, cords, and pseudorosettes (arrow). Hematoxylin and eosin (HE). Inset: Neoplastic cells have strong, intranuclear immunolabeling to Olig2. Immunohistochemistry (IHC.) **Figure 14.** Intraventricular choroid plexus tumor forming cords, tubular-like structures, and pseudorosettes. HE. Inset: Neoplastic cells have diffuse, uniform, strong intracytoplasmic immunolabeling to CKAE1/3. IHC. **Figure 15.** Pituitary corticotroph adenoma associated with the third ventricle forming rosettes, pseudorosettes, and small clusters of neoplastic cells. H&E. Inset: Strong and diffuse cytoplasmic immunolabeling to ACTH. IHC. **Figure 16.** Meningioma forming numerous pseudorosettes and rare meningothelial whorls (arrow). HE.

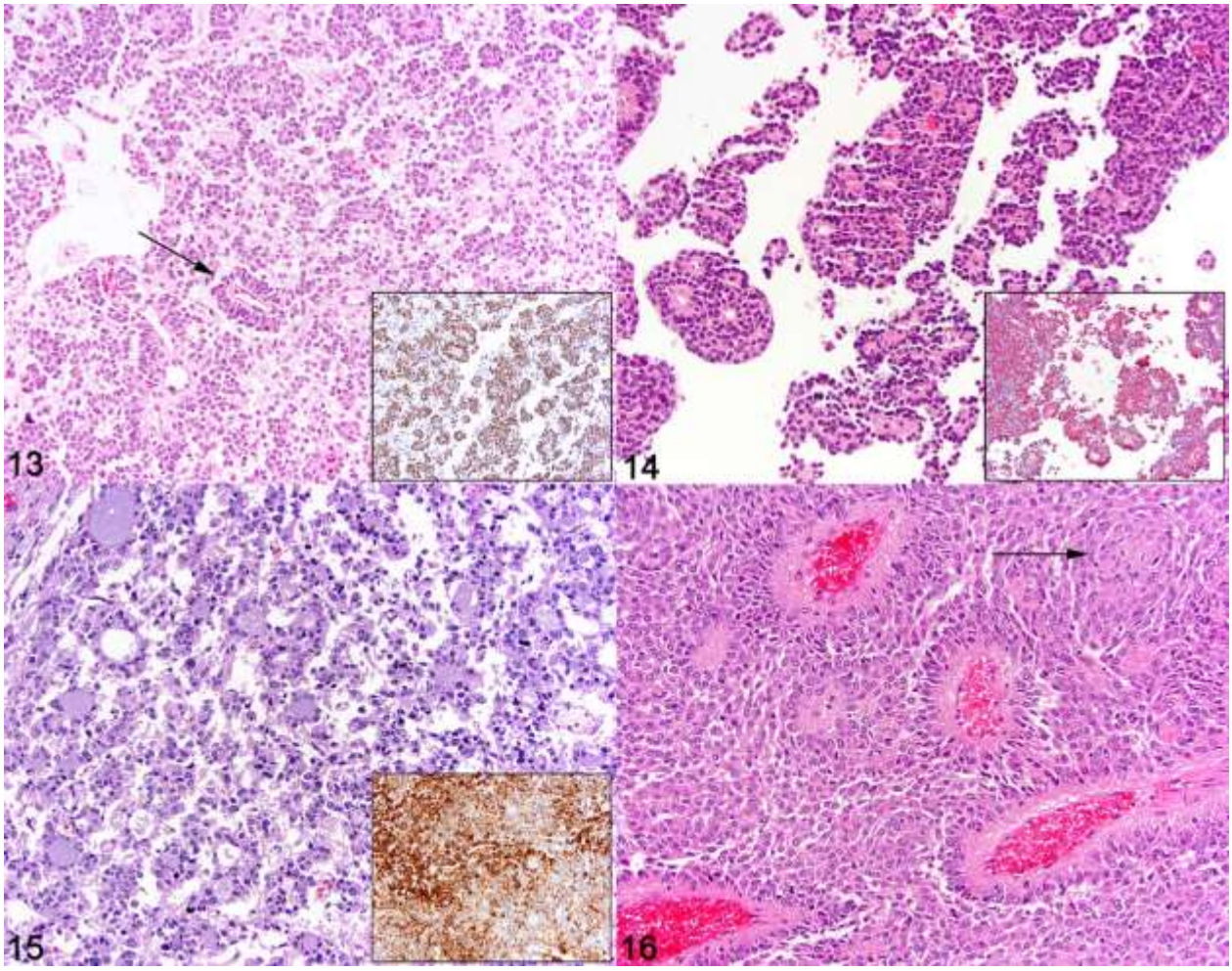

Table 1: Signalment, tumor location, subtype, and immunohistochemical staining profile of cases diagnosed as ependymoma.

Case Number	Breed	Sex	Age (years)	Location and Subtype	GFAP	Olig2	CKAE1/3	S100
1	Pekinese	M	8	Lateral and third ventricle; Papillary	Faint positive	n/a	n/a	Negative
2	Mixed	MC	3	Lateral ventricle, right; Papillary	Faint positive	Rare positive	Positive	Positive
3	Boxer	MI	10	Mesencephalic aqueduct; Tanycytic	n/a	n/a	n/a	n/a
4	Pointer	FS	11	Third ventricle; Papillary	Strongly positive	Rare positive	Positive	Positive

5	Mixed	U	7	Lateral ventricle; Papillary	Strongly positive	Rare positive	Positive	Faint positive

Abbreviations: M = male, not otherwise specified; MC = male castrated; MI = male intact; FS= female spayed; U = unrecorded.